Using low-cost scintillation monitor (ScintPi) measurements to evaluate the elongation of equatorial L-Band scintillation patterns

Isaac G. Wright, Josemaria G. Socola, and Fabiano S. Rodrigues
The University of Texas at Dallas, William B. Hanson Center for Space Sciences, Richardson, TX, E-mail: igw180000@utdallas.edu

ABSTRACT

Irregularities in the ionospheric density are commonly assumed to be elongated along geomagnetic field lines, giving rise to scintillation fading patterns that reflect this elongation. An experiment was carried out in which L-band GNSS signals were measured over the course of nine days using four ScintPi 3.0 scintillation monitors spaced along magnetic east-west and north-south directions at the magnetic equator. Scintillation patterns were found to be greatly elongated in the north-south direction. The extent of elongation was investigated, finding nearly perfect correlation values at a distance of 0.9 km. Likewise, large, but with larger variance, correlations were detected at a distance of 5.8 km, which is, to the authors' knowledge, the longest distance elongation has been investigated since the results reported by Kintner et al. (2004) for a 1 km N-S baseline.

1. GOALS

- Gomez Socola and Rodrigues (2022) developed a low-cost, GNSS-based ionospheric scintillation and Total Electron Content (TEC) monitor. (ScintPi 3.0) .
- They showed that despite the low resolution, 1 dB and 20 Hz, ScintPi 3.0 can provide excellent estimates of scintillation indices (S4).
- We used ScintPi 3.0 to setup an experiment at the magnetic equator to investigate the elongation of L-Band scintillation patterns. The experiment had the following goals:

G1) To evaluate the ability of ScintPi to identify the N-S elongation of scintillation patterns

G2) To compare results obtained with a ~1 km N-S baseline with those obtained by Kintner et al. (2004)

G3) To make new measurements of scintillation pattern elongation for a baseline greater than 1 km.

2. BACKGROUND

- Ionospheric scintillation is an important component of space weather and can be described as rapid fluctuations in the phase and/or amplitude of trans-ionospheric radio signals.
- Ionospheric irregularities are often described as "field-aligned", meaning that electron density perturbations observed, for instance, at the magnetic equator "elongate" along geomagnetic field lines to low latitudes. This is based on the assumption of nearly equipotential field lines. Farley (1959, 1960) provide the theoretical foundation for estimates of the mapping for irregularities of different scale sizes.
- While observations have already confirmed that large scale size irregularities indeed map well along field lines, Kintner et al. (2004) pointed that elongation for irregularities of scale sizes of a few 100s of m (responsible for L-Band scintillation) have yet to be better measured. They setup a low latitude experiment that allowed them to confirm the elongation of L-Band scintillation pattern over a baseline of 1 km in the magnetic N-S direction but indicated that additional observations, particularly with longer baselines, are needed.
- Investigating the shape and orientation of scintillation patterns and how they are cast is important because understanding scintillation can lead to a stronger insight of the characteristics of the ionospheric irregularities that create them.

3. EXPERIMENTAL DESIGN

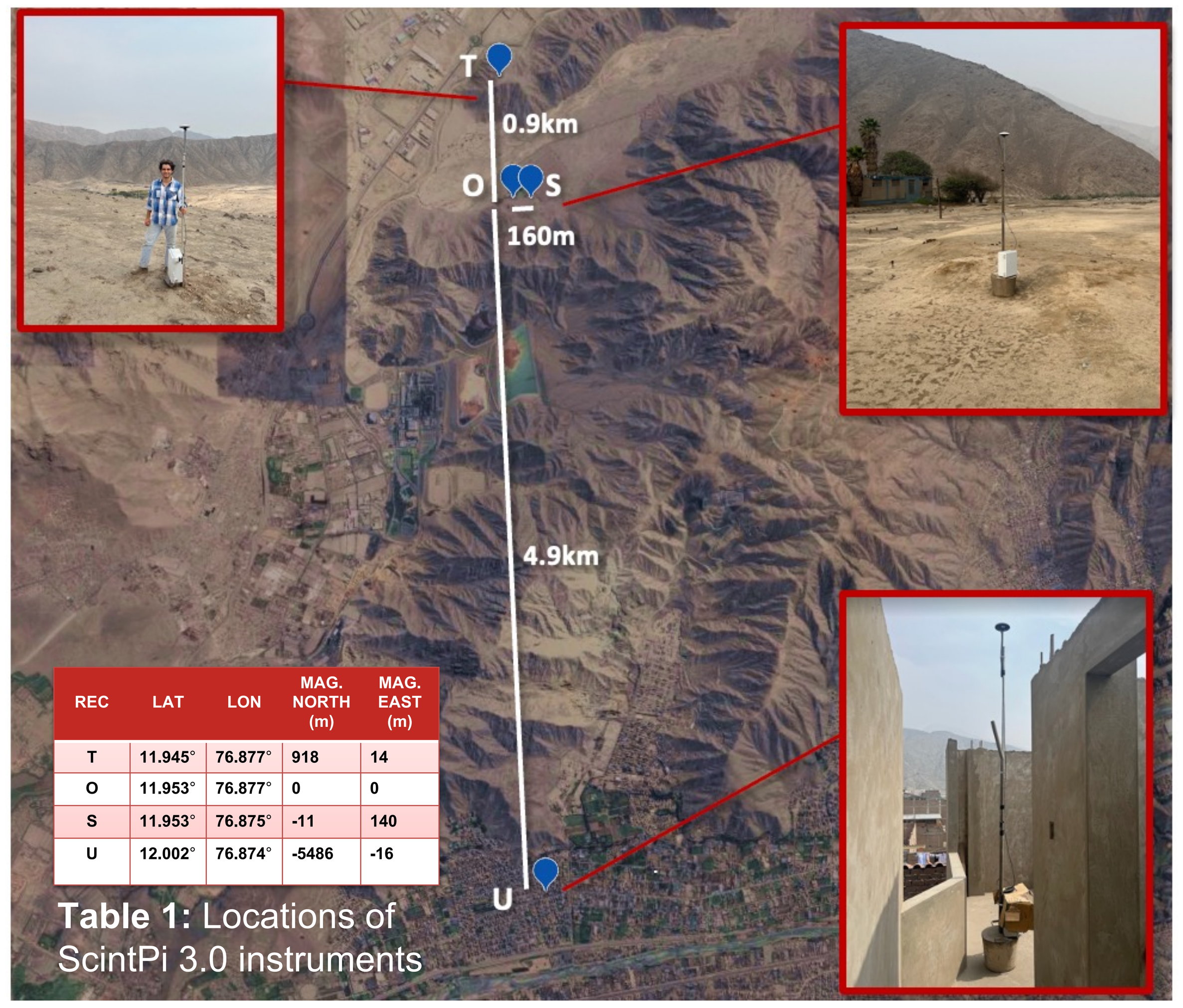

REC	LAT	LON	MAG. NORTH (m)	MAG. EAST (m)
T	11.945°	76.877°	918	14
O	11.953°	76.877°	0	0
S	11.953°	76.875°	-11	140
U	12.002°	76.874°	-5486	-16

Table 1: Locations of ScintPi 3.0 instruments

Figure 1: Map of ScintPi locations with photograph of deployments

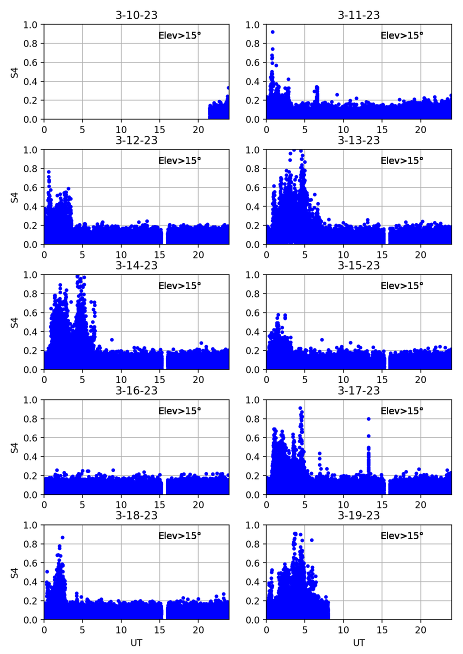

Figure 2: L1 S4 measurements collected by the station U during the March campaign

- GNSS signal measurements at a rate of 20 Hz were made from March 10 to March 19, 2023, near the Jicamarca Radio Observatory in Peru (11.97° S, 76.87° W, and 1.3° dip angle). The measurements were made using an array of four temporary autonomous ScintPi 3.0 stations, labeled T, O, S, and U and shown in **Figure 1** and **Table 1.**

4. METHODOLOGY

- Cross-correlation functions were computed using 60 seconds of L1 C/No measurements where the minimum S4 index was greater than 0.4 and satellite elevation was greater than 15°. **Figure 4** shows an example correlation function for different baselines. **Figure 5** shows examples of signal measurements.
- Because the scintillation patterns evolve in their own reference frame, comparing north-south correlations is fair only when the scintillation pattern is oriented parallel to the receiver pair and when the time delay is relatively small. We consider lags, or τ, where $|\tau| < 5$s.
- Moreover, in general, scintillation surfaces will have different orientations. We will consider the projection angle Φ between the magnetic north-south and the scintillation fade surface, as depicted in **Figure 3**. Using a geometric representation, the projection angle can be calculated from lag times and distances **Eq 1.**

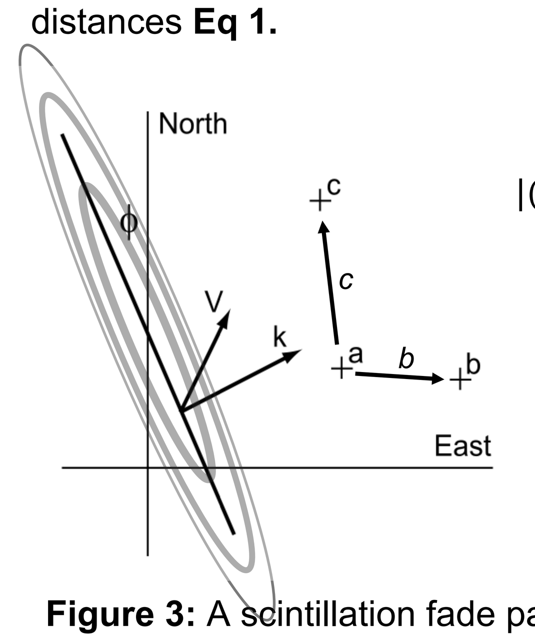

$$\mathbf{k}\cdot\mathbf{r} - \omega\, t = 0$$

$$\omega = \hat{\mathbf{k}}\cdot\mathbf{V}/|\mathbf{k}|$$

$$|(\hat{\mathbf{k}}\cdot\mathbf{r} - \hat{\mathbf{k}}\cdot\mathbf{V}\, t)| = 0$$

$$\hat{\mathbf{k}}\cdot\mathbf{b} - \hat{\mathbf{b}}\cdot\mathbf{V}\, t_b = 0$$

$$\hat{\mathbf{k}}\cdot\mathbf{c} - \hat{\mathbf{c}}\cdot\mathbf{V}\, t_c = 0$$

If **c** is n-s and **b** is e-w:

$$\frac{\sin(\phi)}{\cos(\phi)} = \frac{|\mathbf{b}|t_c}{|\mathbf{c}|t_b} \quad [1]$$

Figure 3: A scintillation fade pattern, represented by phase surface **k**, angle Φ moving with constant velocity **V** across receivers c, a, b. Adapted from Kintner et al. (2004).

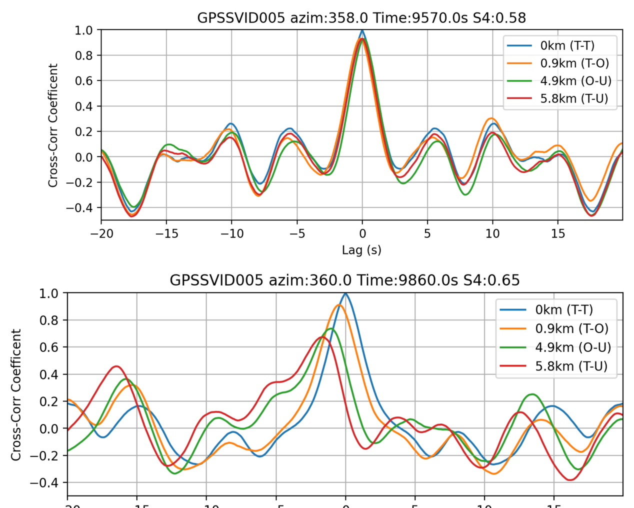

Figure 4: Example cross-correlation functions for (a) when lag times are similar and (b) when lags diverge.

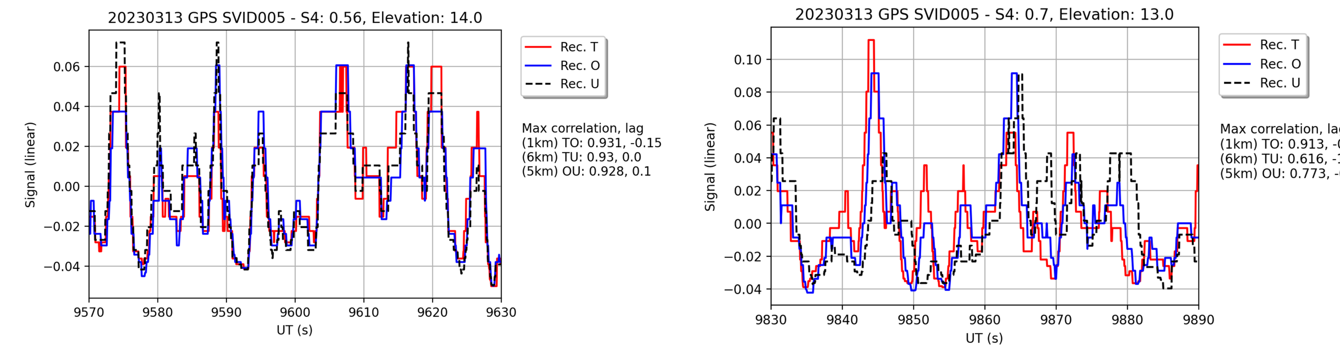

Figure 5: Examples of C/No derived curves for stations T, O, and U when each scintillation pattern has been shifted to the position corresponding to maximal correlation for the correlation functions depicted respectively in figures 4a and 4b.

5. PRELIMINARY RESULTS

5.1 0.9 KM SEPARATION (T-O)

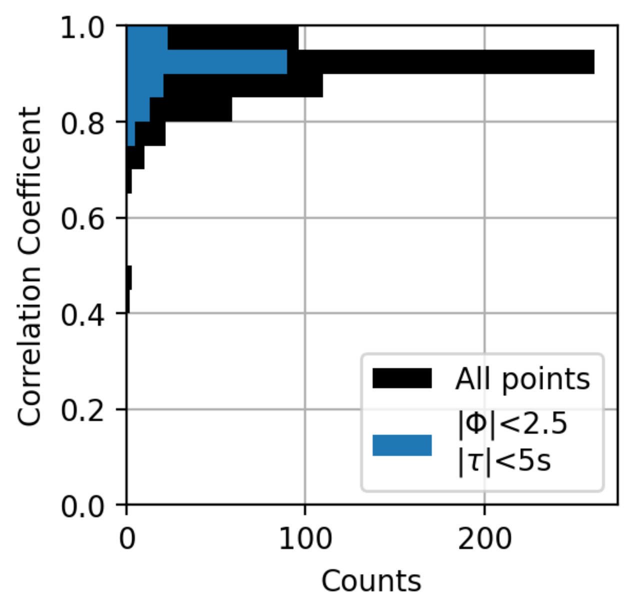

- All points: 607 samples, mean: 0.89, STD: 0.09
- $|\Phi| < 2.5°$, $|\tau| < 5$ seconds: 154 samples, mean: 0.91, STD: 0.05

Figure 6: Count distribution of maximum correlation coefficients for the T-O baseline (0.9 km) for all cases where L1 S4 > 0.4 and elevation > 15° (black), and for cases where $|\Phi| < 2.5°$ and $|\tau| < 5$ seconds (blue).

5.2 5.8 KM SEPARATION (T-U)

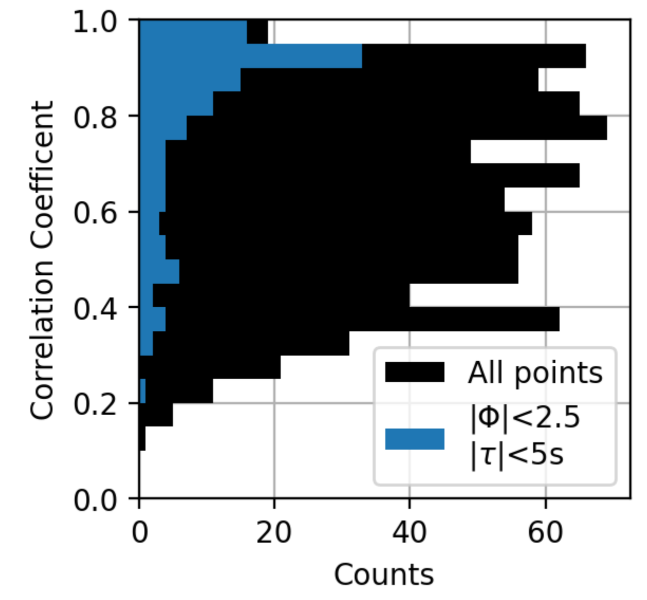

- All points: 787 samples, mean: 0.64, STD: 0.20
- $|\Phi| < 2.5°$, $|\tau| < 5$ seconds: 137 samples, mean: 0.79, STD: 0.19

Figure 7: Count distribution of maximum correlation coefficients for the T-U baseline (5.8km) for all cases where the L1 S4 > 0.4 and elevation > 15° (black), and for cases where $|\Phi| < 2.5°$ and $|\tau| < 5$ seconds (blue).

6. DISCUSSION

G1

- Even before accounting for the projection angle, most of the points (>70%) measured by ScintPis spaced 0.9 km N-S had maximum correlation coefficients of over 0.9. These results are similar to those of Kintner et al (2004) for a similar baseline (1 km). Likewise, a significant portion of the tested points before (10%) and after masking (40%) had maximum correlation coefficients of over 0.9. Because of the prevalence of high correlation values, we conclude that ScintPi is capable of measuring the N-S elongation of scintillation patterns.

G2

- **Figure 8** demonstrates the results of Kintner et al. (2004) elongation analysis. For projection angles within +/-2.5°, the average correlation was 0.967 with a standard deviation 0.045.
- Differences from the expected correlations can be attributed to differences in the selection of data (projection model, bin size, S4 mask) and variations in instrumentation (amplitude resolution & sampling rate) & deployment.
- Nonetheless, we conclude that our experimental results are in good agreement with prior results.

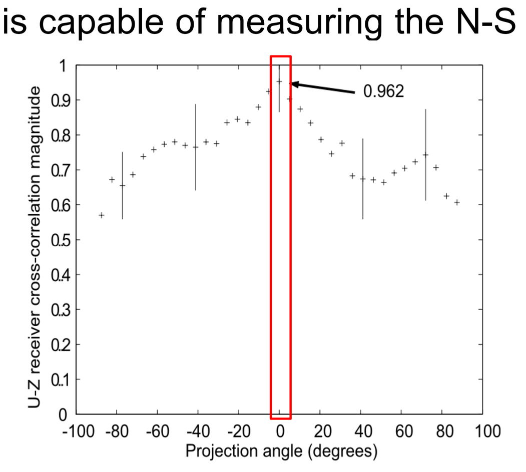

Figure 8: Maximum cross correlation coefficient as a function of projection angle for receivers spaced by 1km NS. Adapted from Kintner et al. (2004).

G3

- We presented a correlation analysis for scintillation measured by receivers separated 5.8 km in the north-south. Considering only small projection angles and lag times skews the distribution of correlation values close to 1. Therefore, we conclude that the elongation of scintillation fading indeed extends to 5.8 km north-south and perhaps much further beyond.
- Due to the high variance of the dataset, it is unclear whether an appreciable change in elongation has been detected from 0.9km to 5.8km. When scintillation patterns are not aligned, the maximum value of the correlation pattern will assume the value at any of the similarly valued peaks, giving nearly random values for the lag time. Therefore, filtering based on lag times can include misidentified points from unaligned scintillation patterns.
- Work is currently being done to improve the selection of data so that only patterns with the same orientation are compared.

7. FUTURE WORK

- Investigate the projection angle as a function of satellite position
- Analyze time duration of scintillation fade
- Measurements beyond 5 km NS

ACKNOWLEDGEMENTS

We would like to thank the staff of the Jicamarca Radio Observatory for technical support. This material is based upon work supported by the NSF Graduate Research Fellowship Program under Grant No. (2136516), by NSF Award AGS-2122639, and by the Eugene McDermott Foundation.

REFERENCES

Farley, D. T., A theory of electrostatic fields in a horizontally stratified ionosphere subject to a vertical magnetic field, *J. Geophys. Res.*, 64(9), 1225–1233, 1959.

Farley, D. T., A theory of electrostatic fields in the ionosphere at non-polar geomagnetic latitudes, *J. Geophys. Res.*, 65(3), 869–877, 1960.

Gomez Socola, J., Rodrigues, F.S. (2022) ScintPi 2.0 and 3.0: low-cost GNSS-based monitors of ionospheric scintillation and total electron content. *Earth Planets Space* **74**, 185.

Kintner, P. M., B. M. Ledvina, E. R. de Paula, and I. J. Kantor (2004), Size, shape, orientation, speed, and duration of GPS equatorial anomaly scintillations, *Radio Sci.*,39, RS2012.

Martinis, C., and Mendillo, M. (2007), Equatorial spread F-related airglow depletions at Arecibo and conjugate observations, J. Geophys. Res., 112, A10310, doi:10.1029/2007JA012403.